Supporting Information

Formation of $CaCO_3$ Fibres Directed by Polypeptide Vesicles

Yingqing Lu, Chunhua Cai,* Jiaping Lin* and Qixin Zhuang

Shanghai Key Laboratory of Advanced Polymeric Materials, State Key Laboratory of Bioreactor Engineering, Key Laboratory for Ultrafine Materials of Ministry of Education, School of Materials Science and Engineering, East China University of Science and Technology, Shanghai 200237, China

* E-mail: jlin@ecust.edu.cn (J. Lin); caichunhua@ecust.edu.cn (C. Cai)

1. Characterization of the PBLG-*b*-PPO-*b*-PBLG and PLGA-*b*-PPO-*b*-PLGA copolymers

The structure of PBLG-*b*-PPO-*b*-PBLG and PLGA-*b*-PPO-*b*-PLGA copolymers was characterized by ^{1}H NMR and GPC. ^{1}H NMR spectra were recorded using Avance 550, Bruker. Figure S1 shows the ^{1}H NMR spectra of PBLG-*b*-PPO-*b*-PBLG and PLGA-*b*-PPO-*b*-PLGA block copolymers using $CDCl_3$ with 15 vol% TFA-d as solvent. Since the degree of polymerization (DP) of the PPO block is known (68), the total molecular weights of the triblock copolymers can be calculated by the peak intensities of the methylene proton signal (5.1 ppm) of polypeptide and the methylene proton signal (3.6 ppm) of PPO in the ^{1}H NMR spectrum (Figure S1a). Compared with the ^{1}H NMR spectrum of PBLG-*b*-PPO-*b*-PBLG, the disappearance of the methylene proton peak (5.1 ppm) in the spectrum of PLGA-*b*-PPO-*b*-PLGA indicates the complete deprotection of the benzyl groups after the hydrolysis reaction (Figure S1b).[S1]

The molecular weight distributions of PBLG-*b*-PPO-*b*-PBLG triblock copolymers with various PBLG block lengths were determined by GPC (Polymer Lab, PL-GPC50) using PBLG homopolymers with narrow molecular weight distribution as standards, performed in DMF/LiBr solution. All the samples show a monomodal GPC curve and narrow molecular weight distribution (Figure S2).

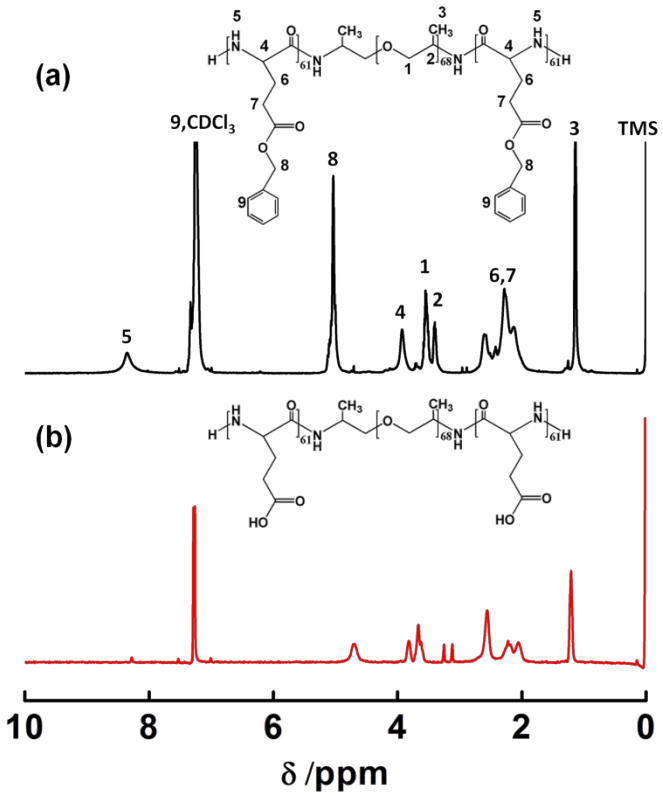

Figure S1 ^{1}H NMR spectra of (a) $PBLG_{61}$-*b*-PPO_{69}-*b*-$PBLG_{61}$ and (b) $PLGA_{61}$-*b*-PPO_{69}-*b*-$PLGA_{61}$ in $CDCl_3$ and TFA-d mixture solvent.

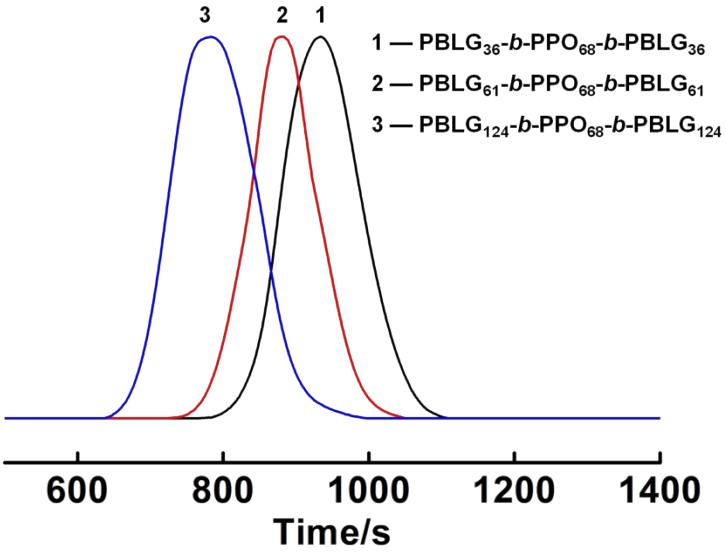

Figure S2 GPC traces of PBLG-*b*-PPO-*b*-PBLG triblock copolymers using DMF/LiBr as eluent.

2. Characterization of vesicles formed in the presence of Ca^{2+}

GPG aggregates with 15 mM Ca^{2+} were examined by laser light scattering and electrophoresis testing, as shown in Table S1. The Ca^{2+} was added in solution at 5 °C. It can be seen that the $<R_g>/<R_h>$ values of the solutions are around 1.0, indicating the vesicular structure of aggregates. The vesicle size is dependent on temperature and copolymer concentration, which is similar to the case of vesicles without Ca^{2+}. The addition of Ca^{2+} can slightly increase the $<R_h>$ values and distributions, which is caused by the binding of Ca^{2+} in vesicle corona. The electrostatic screening effect of Ca^{2+} can decrease the repulsive interaction between PLGA chains in vesicles corona, resulting in the shrinking of the volume occupied by the hydrophilic blocks. Therefore, the interfacial curvature between the PPO and PLGA blocks decreases and larger vesicles are formed. The zeta potentials of GPG-Ca^{2+} vesicles are higher than the vesicles without Ca^{2+}, which indicates the binding effect of Ca^{2+} and COO^- groups.

Table S1 Characteristics of PLGA-*b*-PPO-*b*-PLGA copolymer vesicles

copolymer	Conc. / gL^{-1}	Temp. / °C	$<R_h>$ / nm	PDI[a]	$<R_g>$ / nm	$<R_g>/<R_h>$	ξ / mV
GPG61	1.0	50	152.1	0.12	142.0	0.94	-10.1
GPG61	1.0	35	196.0	0.15	181.6	0.93	-16.0
GPG61	1.0	20	244.6	0.16	260.9	1.07	-20.1
GPG61	0.5	50	106.2	0.10	109.0	1.02	-8.5
GPG61	1.5	50	200.3	0.17	209.9	1.05	-10.8
GPG36	1.0	50	141.4	0.13	140.5	0.99	-12.3
GPG124	1.0	50	170.4	0.14	171.4	1.01	-8.9

[a] Polydispersity index (PDI) of the vesicles was determined at the scattering angle of 90°.

3. $CaCO_3$ crystallization in the presence of PLGA or PPO homopolymers under various temperatures

The influence of PLGA and PPO homopolymers on $CaCO_3$ mineralization was studied as control experiments. The degrees of polymerization of PLGA and PPO homopolymers are 92 and 68, respectively. As shown in Figure S3a-d, smooth spheres were obtained in the presence of PLGA homopolyer. Figure S3e shows the FTIR spectra of the obtained spherical crystals. The absorption bands at 1089, 877, and 745 cm^{-1} are the characteristic bands of vaterite, indicating the crystals are all vaterite at various temperatures. Smooth spheres have been produced in previous literature under the mediation of double hydrophilic block copolymers or acid polypeptides.[S2-S5]

Figure S4 shows SEM images and FTIR spectra of $CaCO_3$ crystals formed under the mediation of PPO homopolymer. The crystals show rhombohedra morphology at various temperatures (Figure S4a-d). In FTIR spectra, the absorption bands at 1089, 877, and 710 cm^{-1} are the characteristic bands of calcite (Figure S4e). The absorption band at 1110 cm^{-1} corresponds to PPO homopolymer, which was probably mixed in crystals because of the low solubility at temperatures above 20 ^{o}C. Rhombohedra particles are usually formed in the absence of additives.[S6,S7] The above results indicate that the influences of PLGA and PPO homopolymer on $CaCO_3$ are independent on temperature.

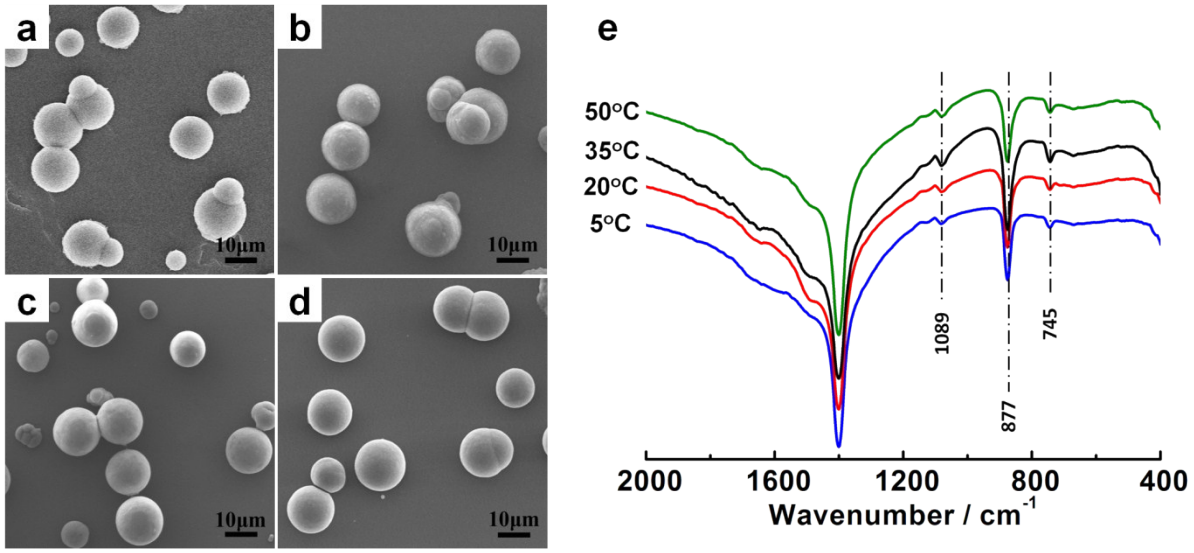

Figure S3 SEM images and FTIR spectra of $CaCO_3$ crystals formed in the presence of $PLGA_{92}$ at various temperatures. (a) 5 °C; (b) 20 °C; (c) 35 °C; (d) 50 °C. (e) FTIR patterns. $[PLGA_{92}] = 1.0\ gL^{-1}$, $[Ca^{2+}] = 15$ mM.

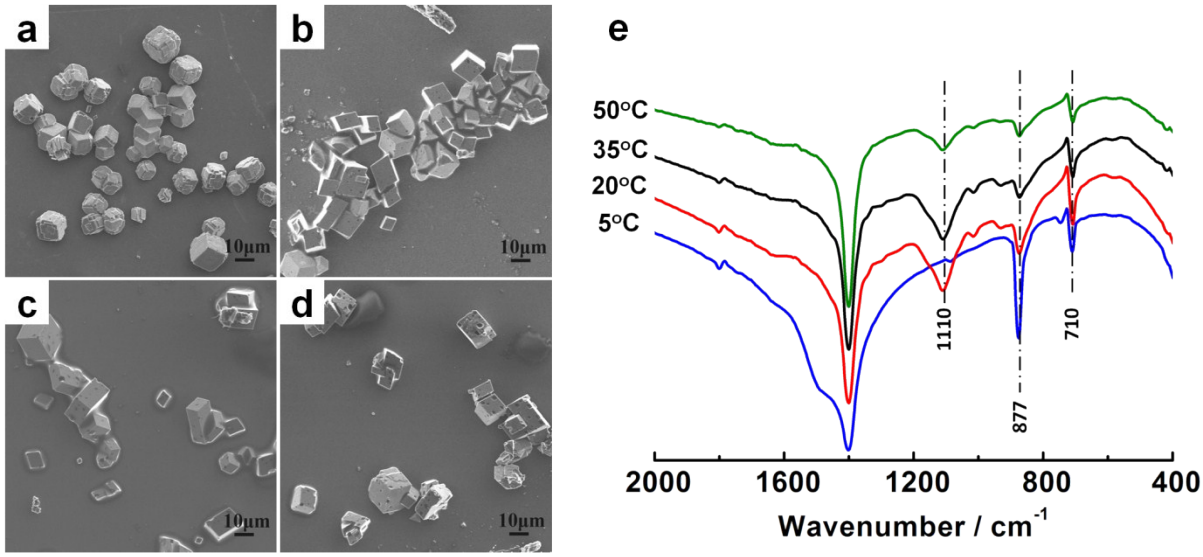

Figure S4 SEM images and FTIR spectra of $CaCO_3$ crystals formed in the presence of PPO_{68} at various temperatures. (a) 5 °C; (b) 20 °C; (c) 35 °C; (d) 50 °C. (e) FTIR patterns. $[PPO_{68}] = 1.0\ gL^{-1}$, $[Ca^{2+}] = 15$ mM.

4. Morphology of reaction intermediates at 20 and 50 °C

The morphologies of amorphous phase at 20 and 50°C are compared by SEM. At 50 °C, the amorphous phase exhibits colloidal-like morphology. The colloidal particles underwent coalescence due to an external forced flow during sample preparation (Figure S5a). At 25 °C, the amorphous particles are solid-like, which show stable spherical shape and cannot fuse with each other (Figure S5c). These two pictures demonstrate the distinct morphology of amorphous phase at different temperatures. Figure S5b shows short fibres formed at 50 °C for 1hr reaction. Most of the fibres contain colloidal-like "bobbles" on the tips. Figure S5d displays crystal patches at 20 °C for 1 hr reaction. The crystallized patches are surrounded by precipitate-free circular halos (as indicated by the arrow). This observation shows that the crystals are formed after ACC via a dissolution/precipitation mechanism.

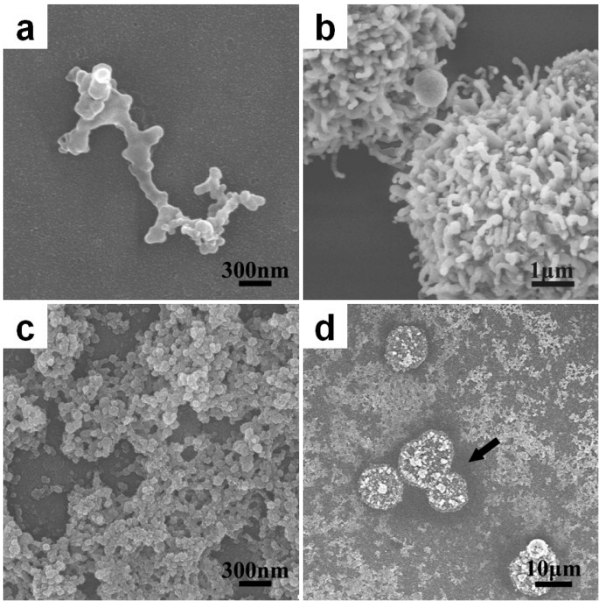

Figure S5 SEM images of intermediates at 20 and 50 °C. (a) Colloidal amorphous precursors formed at 50 °C for 30 min reaction. (b) Crystals formed at 50 °C for 1hr reaction. (c) Solid amorphous particles formed at 20 °C for 30 min reaction. (d) The crystal patches of $CaCO_3$ generated at 20 °C for 1 hr reaction.

5. Investigation of crystal phase transition process at different time intervals at 50, 35, and 20 °C by FT-IR characterization

The structure of reaction intermediates were characterized by FT-IR (Figure S6). The absorption bands at 1654 and 1109 cm^{-1} are attributed to the C=O and C-N stretching vibration bands of GPG copolymer, respectively. These two bands become less evident with time, indicating the decrease of polymer fraction during crystallization. The broad absorption band at 865 cm^{-1} is the characteristic absorption band of amorphous calcium carbonate. The 865 cm^{-1} absorption band vanishes and the ν4 absorption bands of vaterite at 745 cm^{-1} appears at 1hr. After 12 hr reaction, the pattern is unchanged at 50 °C. However, at 35 and 20 °C, the absorption band of calcite at 712 cm^{-1} rises and the band of vaterite becomes weak. This result indicates that the phase transformation process is different at various temperatures. At higher temperature, the calcium carbonate transforms form amorphous to vaterite, and the vaterite is stabilized as the final crystal phase. At lower temperature, the amorphous phase first transforms to vaterite, and then the vaterite crystals continue to transform to calcite.

The polymorph of crystals formed in the absence of additives was examine, as well (Figure S7). Calcite crystals are formed at all temperatures, indicating that temperature cannot change the final polymorph of $CaCO_3$ under this experimental condition. Therefore, the different transformation processes of polymorph in the presence of the vesicles are attributed to the copolymer rather than temperature.

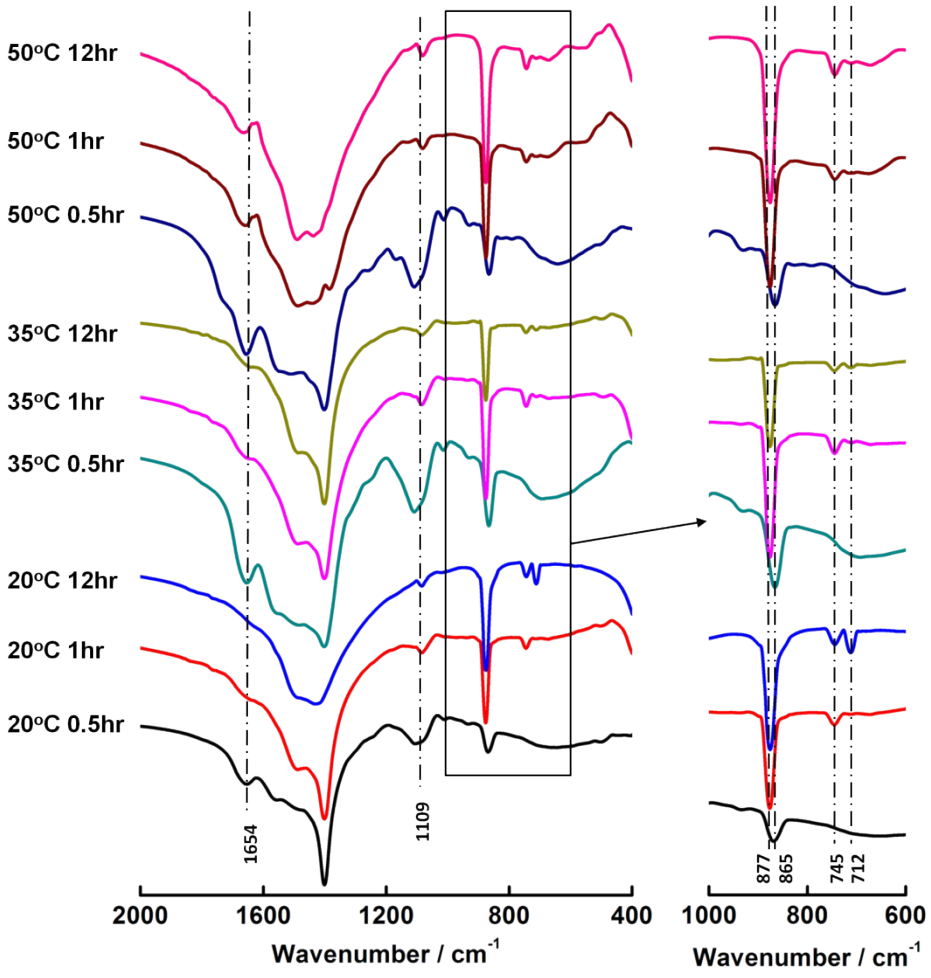

Figure S6 FT-IR spectra of reaction intermediates collected at different reaction intervals at 50, 35, and 20 °C. [GPG60] = 1 gL^{-1}, [Ca^{2+}] = 15 mM.

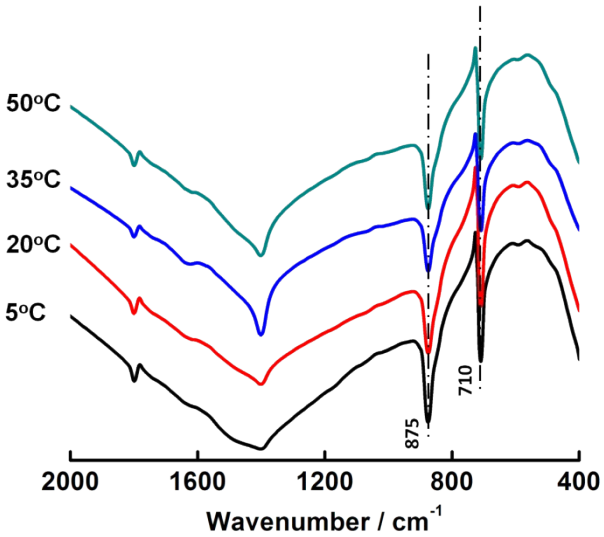

Figure S7 FT-IR spectra of crystals formed at various temperatures in the absence of additives.

References

S1. C. Cai, L. Zhang, J. Lin and L. Wang, *J. Phys. Chem. B*, 2008, **112**, 12666-12673.

S2. X. H. Guo, S. H. Yu and G. B. Cai, *Angew. Chem. Int. Ed.*, 2006, **45**, 3977-3981.

S3. S. H. Yu, H. Cölfen and M. Antonietti, *J. Phys. Chem. B*, 2003, **107**, 7396-7405.

S4. B. Njegić-Džakula, G. Falini, L. Brečević, Ž. Skoko and D. Kralj, *J. Colloid Interface Sci.*, 2010, **343**, 553-563.

S5. R. Kniep and S. Busch, *Angew. Chem. Int. Ed.*, 1996, **35**, 2624-2626.

S6. H. Deng, X. M. Wang, C. Du, X. C. Shen and F. Z. Cui, *Crystengcomm*, 2012, **14**, 6647-6653.

S7. Z. Chen, M. Xin, M. Li, J. Xu, X. Li and X. Chen, *J. Cryst. Growth*, 2014, **404**, 107-115.